URSI GASS 2023, Sapporo, Japan, 19 – 26 August 2023

First results from reconstruction of simulated ionospheric electron density distribution over the Indian region using tomography technique

Ajay Potdar*(1), Ambili KM(1) and R. K. Choudhary (1)
(1) Space Physics Laboratory, Vikram Sarabhai Space Centre, ISRO, Thiruvananthapuram, 695583, https://spl.gov.in/SPL/

Abstract

We present a mathematical tomographic technique to map three-dimensional electron density distribution in the ionosphere over the Indian region in a specified volume grid. This technique utilizes the Slant Total Electron Content (STEC) data from multi-frequency receivers and Global Positioning System (GPS) satellites placed over predetermined locations in India, in real-time. In order to validate the results, we have developed a simulation to emulate real time scenario of GPS satellite orbital tracks with respect to receiver locations corresponding to an hour with a sampling rate of 1 minute. As a substitute for the real electron density distribution, we use electron density obtained from the IRI model for our scenario, from which TEC values are derived and subsequent reconstruction is done to get the electron density distribution.

1. Introduction

Electron density in the ionosphere has been of interest to the scientific community since the dawn of radio communication. Earlier in-situ measurements included vertical profiles of electron densities using rocket-borne experiments which are limited to the maximum height of the rocket and ionosondes which are able to probe till the F2 peak electron density layer [1]. With the advent of technology, remote sensing observations using RADAR were used to probe the ionosphere till a higher altitude of 1000 km, but comes at great logistical costs. As the number of satellites increased, radio communication was also utilized for more sophisticated scientific studies. Subsequently, space weather impact on satellites and radio communication was observed. Electron density distribution and its temporal variation was understood to be an important aspect contributing to the received signal strength and scintillation effects in radio communication. In order to study these dynamics in the ionosphere, computerized tomography was first pioneered by [2] and employed over the years in the community. The approach by [2] was based on an iterative mathematical technique to image the real-time ionosphere by combining and operating on a set of total electron (TEC) content values.

In this paper, we present one such development of the technique for application in the Indian region. The following section discusses the data required for the analysis. We then introduce voxels and describe their utility along with the Algebraic Reconstruction Technique in mapping the ionosphere, finally presenting preliminary results.

2. Observations and Data

TEC is defined as the line-of-sight path integral of electron density between a transmitter and a receiver. This parameter is indirectly calculated using GNSS multi-frequency receivers which are placed strategically on the ground. The GNSS receivers primarily record the ionospheric delay from the difference between the pseudorange and the carrier phase of two carrier signals of frequencies L1 (1575.42 MHz) and L2 (1227.6 MHz) for GPS satellites. The multi-frequency receivers also log the coordinates of the transmitting satellites, the receiver station, as well as the time in UTC at 1 Hz frequency in the form of binary data which is extracted for further processing. The STEC values are calculated from the ionospheric delay values using the following expression:

$$I_f = \frac{40.3}{f^2} TEC$$

where, I_f is the Ionospheric delay, f is the frequency. This data is required by the tomography algorithm as described in the following section.

3. Methodology

3.1 Voxels

The technique presented here is used to reconstruct the real-time ionosphere profile of electron density, in discrete elements of a 3-dimensional grid, the smallest element of which is called a voxel and the grid is specifically called a voxel grid. This voxel grid is defined by mathematical boundaries which are functions of latitudes, longitudes, and heights in the World Geodetic System (WGS-84) reference frame. The voxel grid is confined in spatial extent as well as assigned a resolution based on our requirements as well as limitations. These voxels are assigned an index each, starting from 1 to m, m being the total number of voxels (Figure 1) and respective values of electron densities. We assume that the electron density in a voxel is constant throughout. We intend to find a solution for the variable set: $[n_1, n_2, n_3 \ldots . n_{24}] = N$ essentially reconstructing the electron density profile 3D space.

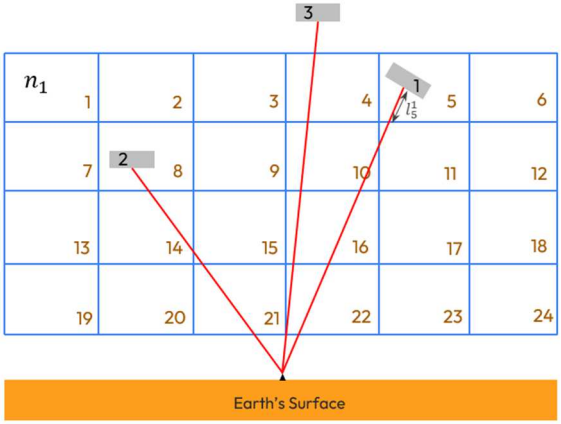

Figure 1. Example of voxel grid and satellite ray paths for illustrative purpose. The small triangle in black is a receiver and the grey rectangles are satellites. The blue grid displays a side view of a 3-dimensional voxel grid.

The computerized tomography technique operates on a set of linear equations to obtain the solution. In order to obtain a linear equation, we need a TEC value observation corresponding to which we have one receiver and one satellite coordinates at a given time. This TEC value is assumed to be the sum of product of length in each voxel and the electron density in each voxel along the ray along the line of sight of the receiver and the transmitter (Figure 1). A compilation of such observations, from available satellites and receiver paths are combined together as given below:

$$TEC_1 = n_5 {l_5}^1 + n_{11} {l_{11}}^1 + n_{10} {l_{10}}^1 + n_{16} {l_{16}}^1 + n_{22} {l_{22}}^1$$

$$TEC_2 = n_4 {l_4}^2 + n_{10} {l_{10}}^2 + n_{16} {l_{16}}^2 + n_{22} {l_{22}}^2$$

$$TEC_3 = n_8 {l_8}^3 + n_{14} {l_{14}}^3 + n_{15} {l_{15}}^3 + n_{21} {l_{21}}^3$$

...

Where, TEC_a is the observed TEC value along the a^{th} receiver, and satellite position instance and ${l_b}^a$ is the length of the ray in the b^{th} voxel. An accumulation of this data gives a set of linear equations to solve, which when converted into matrix form are as follows:

$$\begin{bmatrix} TEC_1 \\ TEC_2 \\ TEC_3 \\ .. \\ TEC_m \end{bmatrix} = \begin{bmatrix} l_1^1 & l_2^1 .. & l_{24}^1 \\ l_1^2 & l_2^2 .. & l_{24}^2 \\ l_1^3 & l_2^3 .. & l_{24}^3 \\ .. & .. .. & .. \\ l_1^m & l_2^m .. & l_{24}^m \end{bmatrix} \begin{bmatrix} n_1 \\ n_2 \\ n_3 \\ .. \\ n_{24} \end{bmatrix}$$

$$TEC = LN$$

Note that the number of equations is typically more than the number of variables in such studies. Algebraic reconstruction techniques offer a solution to this problem with their iterative nature. A brief description of their implementation is given in the following section.

3.2 Algebraic reconstruction

The Algebraic Reconstruction Technique (ART) was developed for medical applications to probe human organs non-destructively. It is capable of handling a set of linear equations, in order to obtain a solution when the number of equations are greater than or equal to the number of variables which is generally the case with studies similar to this. The technique is iterative in nature, requiring an *a priori* solution. The *a priori* set of values for N is generally taken as rough approximation of the solution, and can be obtained from models, as well as data of a prior observation. The iteration is halted and the solution is accepted when the following condition for N, in the k^{th} iteration is satisfied:

$$|N^{k+1} - N^k| < \tau$$

where, τ is the defined acceptable error. To compute the solution N^k, we employ the Simultaneous Multiplicative Algebraic Reconstruction Technique (SMART) which is a modified equation from [3] and given as:

$$N^{k+1} = N^k \left[\prod_{m}^{i=1} \left(\frac{TEC_i}{L^i \cdot N^k} \right)^{\frac{L^i}{\max(L)}} \right]^{\frac{1}{m}}$$

where, N is the set of electron density value of all the voxels, k is the iteration no., L^i is the i^{th} row of the L matrix.

4. Simulation

In order to simulate reconstruction of the electron density tomogram we assume an electron density distribution from the IRI model (International Reference Ionosphere) averaged over an hour. This is done considering a voxel grid with a resolution of 3^o latitude × 3^o longitude × 190 km height centered at coordinates 22^o latitude and 83^o longitude and is displayed in Figure 2.

For the *a priori* electron density distribution, we used the IRI model, but computed for an hour before that of the assumed IRI model. The underlying assumption here is that electron density distribution does not change significantly within an hour [4]. This allows us to utilize TEC observations from a satellite in time sample interval of one minute, across the receiver field of view, in its orbit and covering more number of voxels in the grid. Hence, the GPS satellite coordinates, the latitude and longitudinal extent of which are constrained through the field of view allowed by the voxel grid for the ground receivers, are also computed over an hour and are depicted in Figure 3 in red tracks. From these coordinates in addition to the assumed

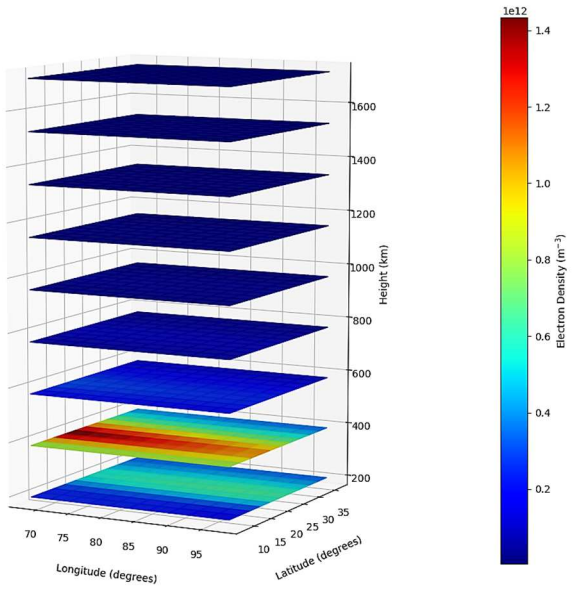

Figure 2. Assumed electron density distribution.

electron density distribution, the TEC values are calculated by determining the ray path equations and corresponding length in a given voxel, for every combination of satellite and receiver position.

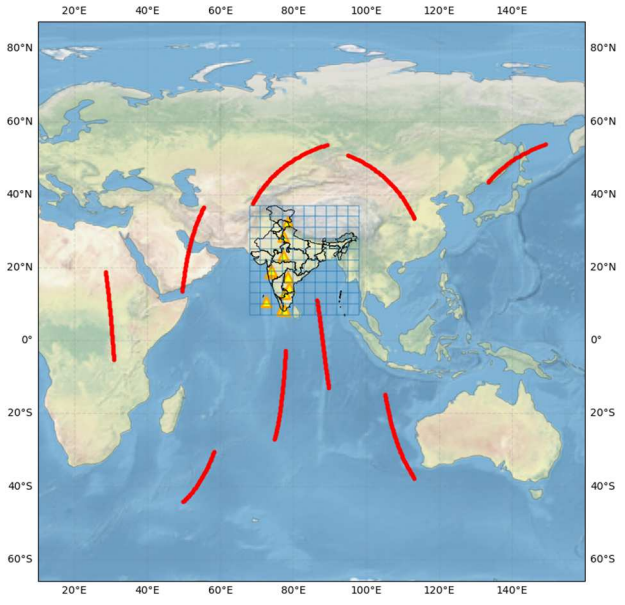

Figure 3. Top view of the voxel grid in light blue gridlines, with GPS satellite tracks over 1 hour in red and receiver positions in yellow.

In a real world scenario, with limitations on receiver positions, the voxel grid will not be intersected completely, essentially affecting the accuracy of the reconstructed tomogram. Given in Figure 4 is the coverage of ray paths and corresponding intersected voxels. The voxels which have zero ray paths crossing them are represented in red. We observe that, at lower heights the number of voxels with zero intersections is higher but decreases with respect to height. This is due to the movement of satellites which

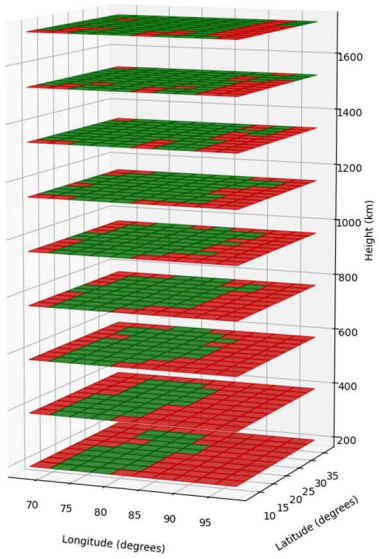

Figure 4. Voxel intersection matrix depicting voxels with more than one ray path intersection in green and voxels with no intersection in red.

essentially sweeps the ray paths at a higher velocity at higher altitudes. From the previous steps and the implementation of the SMART algorithm, we obtain the reconstructed electron density distribution for $\tau = 10^7\ \mathrm{m}^{-3}$ as displayed in Figure 5.

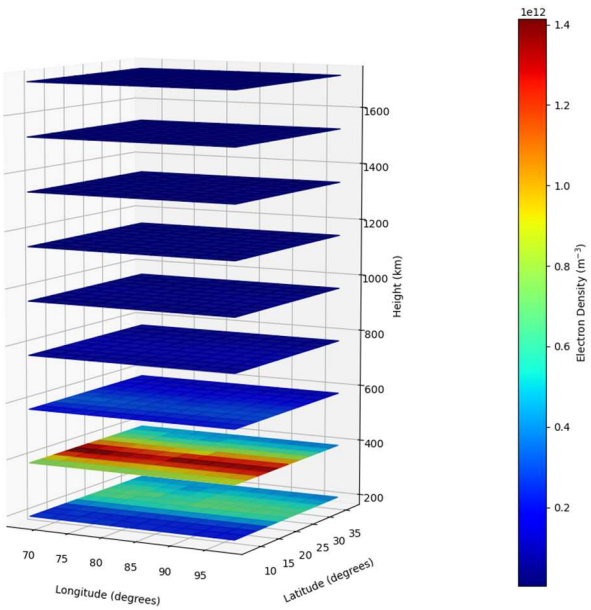

Figure 5. Reconstructed electron density distribution.

The reconstructed tomogram is agreeable with the assumed electron density distribution, with errors (Figure 6) within permissible limits of 28%. The high values of errors are in the voxels which have few ray crossings. A significant portion of the tomogram has less error than 10% and can be considered reliable.

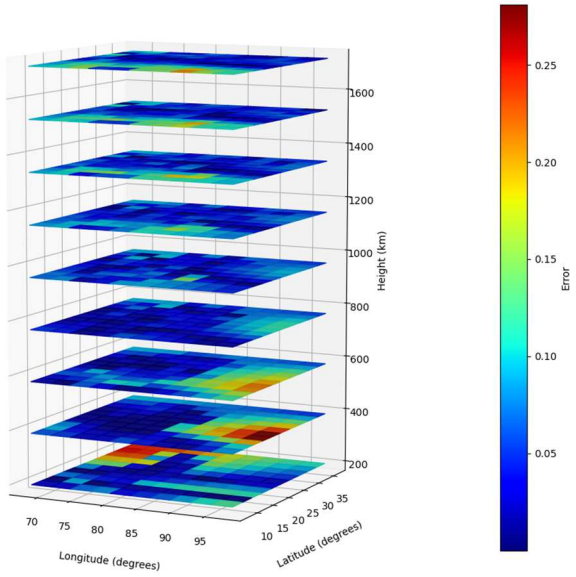

Figure 6. Error matrix of the reconstructed tomogram. The error matrix is computed as: $Error^j = \frac{N_{rec}^j - N_{IRI}^j}{N_{IRI}^j}$, where, j is the voxel index and N_{rec} and N_{IRI} are the electron density vectors of the reconstructed and the IRI model assumed distribution, respectively.

The overall tomogram, is acceptable for analysis and further studies and the capability for such tomograms to be reconstructed in real scenarios with TEC data from multi-frequency, multi-satellite GNSS receivers is achieved. A few caveats here are the low spatial and temporal resolution of the voxel grid as well as limited coverage due to dependence on receiver positions. The ART techniques modify only those voxel electron density values for which it has information of and are involved in observations. One solution to the issue is using a denser receiver populated over a larger area considering the voxel grid. A mobile receiver platform aboard an aircraft or even in LEO can also be implemented for a wider coverage. Incorporation of VTEC maps in regions not covered is also a feasible solution. These modifications can improve the resolution of the tomogram which can subsequently be used to study the ionosphere and its dynamics.

5. Summary

We have validated our technique of using the SMART algorithm to reconstruct the real time ionospheric electron density using GPS TEC observations simulated using an assumed electron density distribution in a three dimensional voxel grid. The reconstructed tomogram is in fair agreement with the assumed electron density distribution and with increasing receivers in the field a more accurate tomogram can be obtained.

6. Acknowledgements

The authors acknowledge the help and support of Director, SPL in formulating the program and implementing it.

7. References

1. Radicella, Sandro M., and Yenca O. Migoya-Orué. "GNSS-derived data for the study of the ionosphere." GPS and GNSS Technology in Geosciences. Elsevier, 2021. 221-239.

2. Jeffrey R Austen, Steven J Franke, and CH Liu. Ionospheric imaging using computerized tomography. Radio science, 23(03):299–307, 1988.

3. Bust, Gary S., and Cathryn N. Mitchell. "History, current state, and future directions of ionospheric imaging." Reviews of Geophysics 46.1 (2008).

4. Fabricio dos Santos Prol, Timothy Kodikara, Mohammed Mainul Hoque, and Claudia Borries. Global-scale ionospheric tomography during the march 17, 2015 geomagnetic storm. Space Weather, 19(12): e2021SW002889, 2021.